Available online at www.sciencedirect.com
SCIENCE DIRECT
Chemical Physics 323 (2006) 149–160
Chemical Physics
www.elsevier.com/locate/chemphys

Femtosecond study of light-induced fluorescence increase of the dark chromoprotein asFP595

Tanja A. Schüttrigkeit [a,1], Till von Feilitzsch [a,1], Christian K. Kompa [a], Konstantin A. Lukyanov [b], Alexander P. Savitsky [c], Alexander A. Voityuk [d], Maria E. Michel-Beyerle [a,*]

[a] Department Chemie, Technische Universität München, 85747 Garching, Germany
[b] Shemiakin and Ovchinnikov Institute of Bioorganic Chemistry, Russian Academy of Sciences, Moscow, Russia
[c] A.N. Bach Institute of Biochemistry, Russian Academy of Sciences, Moscow, Russia
[d] Institució Catalana de Recerca i Estudis Avançats (ICREA), Institute of Computational Chemistry, Universitat de Girona, Spain

Received 19 May 2005; accepted 13 September 2005
Available online 3 November 2005

Abstract

Femtosecond time-resolved spectroscopy is applied to study the mechanism of the light-induced increase of fluorescence quantum yield of the initially non-fluorescent (dark) chromoprotein asFP595. Spectroscopic and kinetic characteristics of this unique fluorescence "kindling" phenomenon are: (i) the small Stokes shift of the dark chromophore consistent with either the zwitterion or the anion; (ii) the singlet excited state of the dark chromophore decaying predominantly with a time constant of ~320 fs corresponding to a fluorescence quantum yield $\Phi_{Fl} \leqslant 10^{-4}$. Since ground state recovery occurs on the same time scale, this radiationless channel is assigned to internal conversion; (iii) the formation of the fluorescent species depending on the sequential absorption of two photons with a delay significantly exceeding the excitation pulse duration of 150 fs; (iv) the fluorescent species showing a red-shift of ~20 nm in absorption and emission, and an excited state lifetime of 2.2 ns. The ultrafast internal conversion of the excited dark state is attributed to the proximity of the S_0 and S_1 potential energy surfaces favored by the non-planarity of the chromophore as revealed in recent X-ray structures. Competing with internal conversion two different transformations of the chromophore structure are suggested which may be identified in a future X-ray structural analysis of the the photoconverted fluorescent state. The predominant kindling mechanism may be either (i) *trans–cis* isomerization or (ii) proton transfer between an excited zwitterion and the protein cleft. For mechanism (ii) the large dipole moment change of about 11 D upon S_0–S_1 excitation of the chromophore would be crucial in order to initiate protein relaxation and deprotonation of a zwitterion. Both mechanisms are assumed to lead to a metastable planar structure responsible for the long-lived fluorescence of the chromophore "kindled" at high light intensities.

Keywords: asFP595; Red fluorescent protein; Femtosecond spectroscopy; Fluorescence kindling mechanism

1. Introduction

Fluorescent proteins (FPs) are ubiquitously used as non-invasive fluorescence markers for gene expression and protein localization in cell and molecular biology and as biosensors [1,2]. These proteins have gained unprecedented popularity due to their key properties that they may be heterologically expressed in living cells [3], that no additional enzymes or cofactors are needed to produce fluorescence signals, and that they do not interfere with the marked protein in fusion tags. In principle, all these applications depend on a high quantum yield of fluorescence or on its control by external parameters. In fact, a quantum yield close to unity ($\Phi_{Fl} = 0.8$ [4]) is the fingerprint of the

* Corresponding author. Fax: +49 89 289 13026.
E-mail address: michel-beyerle@ch.tum.de (M.E. Michel-Beyerle).
[1] Authors contributing equally to this publication.

0301-0104/$ - see front matter © 2005 Elsevier B.V. All rights reserved.
doi:10.1016/j.chemphys.2005.09.039

FP "pioneer", the green fluorescent protein (GFP) where the chromophore is tightly fixed in a planar *cis*-conformation inside a can-shaped protein [5,6]. This high quantum yield is lost upon protease digestion or heat denaturation and, most interestingly, also in some mutants with blue or red-shifted emission [7,8]. Therefore, elucidation of the radiationless deactivation mechanisms in these non- or weakly fluorescing proteins is of central importance for the development of mutagenetic strategies.

The chromophore (4-*p*-hydroxybenzylidene-imidazolidin-5-one) in wt-GFP is formed autocatalytically by post-translational cyclization–dehydration oxidation of Ser65, Tyr66 and Gly67 [7–9]. Within the protein, the chromophore is present in two protonation forms, a neutral state ROH carrying the protonated Tyr66 and its deprotonated anion RO^- [10,11]. Excitation of ROH in its maximum at 397 nm leads to the green fluorescence peaking at 508 nm. This apparently large Stokes shift of 5600 cm^{-1} originates from a conformationally unrelaxed anionic state formed upon excited state proton transfer (ESPT) and stabilized through a hydrogen bond network from (ROH)* to Glu222. Such a hydrogen bond network does not exist for the conformationally relaxed anionic ground state RO^-.

In contrast to wt-GFP, there are non-fluorescent mutants where the fast dynamics of the excited state does not lead to an intermediate, but to the direct recovery of the ground state [12–14]. This behavior is a fingerprint of internal conversion, being the dominant radiationless process, independent of the protonation state of the chromophores. For comparison, the time constant of internal conversion of the GFP chromophore free in solution has been shown to be even faster, i.e., in the sub-picosecond range. It is determined by rotational motion within the chromophore involving the exocyclic ═CH═ group which connects the aromatic ring with a heterocycle [15,16]. Obviously, a crucial condition for high fluorescence quantum yield is the restriction of motional freedom in this linking element. Surprisingly, molecular mechanics simulations [17] have demonstrated that the space requirements for aromatic ring rotation are indeed met in the GFP chromophore since the cavity around the chromophore is complementary to an excited state conformation in which the phenol and imidazolidinone rings are perpendicular to each other. Thus, it is not necessary to invoke hula twisting in search of a less space-consuming mode of motion. Moreover, internal conversion depends not only on the motional freedom given by the geometry of the binding pocket but also on the hydrogen bonds the chromophore may form [12–14]. Independent of the topic of this paper, a deep understanding of radiationless processes in GFP-type chromophores would be helpful for the optimization of GFP-based molecular sensors, which probe both, the hydrogen bond network around the chromophore and the rigidity of the binding site.

Another intriguing feature of some GFP mutants related to non-fluorescent states of the chromophore is "on–off blinking", discovered in single molecule spectroscopy [18] and studied extensively utilizing also other methods [19,20]. Here the fluorescent GFP chromophore in its "on"-state may reversibly transform to a non-emissive state ("off"-state) with a lifetime up to several seconds. The duration of the "on"-state decreases with increasing intensity [19–21] up to converting the entire population into the dark "off"-state [22]. The molecular nature of "on–off" blinking and photoreversible switching between fluorescent and non-fluorescent states has been related to diverse processes as photoinduced isomerization [23,24] and changes in the chromophore's protonation states [18,19,25]. Quantum chemical calculations attribute the dark "off"-state to a zwitterionic species formed by proton transfer from the nearby glutamate (Glu222) to the nitrogen of the heterocyclic ring of the anionic chromophore in its excited state $(RO^-)^*$ [26].

In theoretical approaches the evolution of excited state relaxation of the GFP chromophore has been investigated through potential energy surface scans [27–31]. The torsional coordinates describing the twisting of the tyrosyl ring around the C_2–C_3 and C_3–C_4 bridging bonds (see molecular Scheme 1 in Section 4) were considered as relaxation coordinates and the S_1 and S_0 potential energy surfaces spanned by these twisting modes have been analyzed for different protonation states of the chromophore. It turns out that the zwitterionic state of the chromophore exhibits the smallest energy gap between the S_1 and S_0 potential energy surfaces. Since this energetic proximity of the two potential energy surfaces in the vicinity of a conical intersection sets the scene for efficient internal conversion [32], the dark state has been assigned to the zwitterion [26]. As a result, for energetic reasons in the singlet excited zwitterion, internal conversion may well be the predominant decay channel leading to fast recovery of the electronic ground state.

For the chromoprotein asFP595, which provides the intense purple color to the tentacle tips of the sea anemony *Anemonia sulcata*, a novel and so far unique phenomenon has been reported [33]. At low light intensities these tentacles are non-fluorescent, corresponding to a fluorescence quantum yield of $\Phi_{Fl} < 0.001$, that has been shown to depend critically on the nature of specific amino acid residues in the chromophore's environment [33–35]. However most surprisingly, high intensity irradiation with green light leads to a drastic increase of Φ_{Fl}. This phenomenon termed fluorescence "kindling" [33,34] is reversible since in the dark, the chromophore returns (within a characteristic time of 10 s [33]) to its initial non-fluorescent state. Alternatively, the kindling phenomenon can be instantly reversed by irradiation with blue light [33–35] in response to an absorption band at 450 nm reported for the fluorescent state [34]. In the absence of more detailed experiments and structural information the kindling mechanism has been related to conformational changes [34,35].

The kindling properties of asFP595 can be optimized by the inclusion of the mutation Ala148Gly to produce

the variant KFP (kindling FP), in which the dark recovery time is slowed down to 100 s at 295 K [34,35]. Recently, the crystal structure of this variant in its dark state has been determined to 2.1 Å resolution [36]. The most prominent features of the crystallographic data, in which KFP differs from GFP are the following ones: (i) an extension of the π-system of the chromophore comprising a *p*-hydroxybenzylidene-imidazolinone moiety being responsible for the red-shift of the absorption spectrum; (ii) the chromophore adopting a non-planar *trans* conformation within the interior of a GFP-type β-can, and (iii) a main chain cleavage of the polypeptide backbone at one end of the chromophore in line with previous results [37]. Shortly after this crystal structure analysis and after completion of this paper, a high-resolution structure (1.38 Å) of KFP appeared [38]. Aside from minor differences in the conformation of surface residues, the features (i) to (iii) of the two structures (termed in the following A [36] and B [38]) are qualitatively similar. Similarities include also the hydrogen bonds between the chromophore and amino acid side chains of the binding pocket as Glu215, Arg92, Ser158 and of water. Differences relate mainly to the location of His197 and the potential role of this side chain in the kindling mechanism [38] as well as to less important details of the chromophore structure. First, in structure A an imino group extends the chromophore's π-system while in structure B a single carbonyl group is sufficient to provide the strong bathochromic shift of the absorption spectrum. We note in passing, that the chromophores in structure B and in the red fluorescent protein dsRed [39] are identical. The chemical structure of chromophore B is further supported by the spectroscopic characteristics of a model compound in solution, which closely matches the chromophore of KFP [40]. Second, the deviation from planarity is significantly more pronounced for the chromophore of structure A as compared to structure B. However, this discrepancy might be related to the low temperature (100 K) conditions of the X-ray structural analysis B.

Reversible transitions between fluorescent and dark states are of broad interest, as they may eventually be exploited in the growing field of information storage in macromolecules or as active labels in biological systems. Thus, it is the goal of this paper to apply femtosecond to picosecond time-resolved spectroscopy to the investigation of the dynamics and the mechanism of fluorescence kindling in the dark chromoprotein asFP595 and interpret the results in the light of theoretical considerations based on the recent X-ray structures [36,38]. As the position 148 has been shown to be of utmost relevance for the low fluorescence quantum yield of asFP595 [41], time-resolved studies are extended to the single site mutant asFP595–Ala148Ser. In this mutant, the fluorescence quantum yield of $\Phi_{Fl} = 0.012$ is by more than a factor of 10 higher than the one of wt-asFP595 [33], while the phenomenon of fluorescence kindling is persisting.

2. Experimental details

2.1. Preparation of the chromoprotein asFP595

The red chromoprotein asFP595 was obtained according to the protocol described previously [33,42]. The full-length coding region of asFP595 was cloned into a pQE30 vector (Qiagen). The wild type protein as well as its Ala148Ser mutant were expressed in *Escherichia coli* with a 6× His tag at the N-terminus and purified using TALON metal-affinity resine (Clontech). As controlled by electrophoresis, the purity of all preparations of the heterologous expression products was better than 95%. In order to perform low temperature spectroscopy, the protein was dissolved in a mixture of glycerol (60%) and glycine buffer (pH 8, 50 mM, 40%). For steady-state measurements at low excitation intensities the protein concentration is adjusted to yield an OD_{max} of 0.3 in a 1 mm quartz cuvette. For the high intensity measurements OD_{max} is 0.22 in a quartz cuvette with 1 cm path-length.

2.2. Spectroscopic methods

2.2.1. Steady-state spectroscopy

Low intensity absorption spectra were recorded with an UV–Vis spectrometer (Perkin–Elmer Lambda 2S) with a spectral resolution of 2.0 nm or better. The respective fluorescence spectra were measured using a spectrofluorometer (Spex Fluorolog-2 Model F212I). In order to overcome the negligible fluorescence quantum yield, a 4 mm path-length quartz cuvette was used and the entrance/exit slits of the monochromators were set to 5 mm allowing for highest sensitivity at the expense of spectral resolution which was then limited to ca. 7 nm. For low temperature experiments a liquid nitrogen-cooled continuous-flow cryostat (Leybold VSK 3-300) was integrated into the spectrometer.

High intensity fluorescence spectra were taken after excitation with an Ar^+-laser system operated in cw mode at 514 nm, reaching a maximal power $P \sim 100$ mW. Since the excitation beam (~10 mm diameter) was focused onto the sample using a $f = 200$ mm lens, the minimal radius of the excitation beam was ~1.5 μm. Taking into account the width of the cuvette (10 mm), an effective average beam diameter of about 0.1 mm is estimated. For the maximal power of ~100 mW this corresponds to a photon flux 3×10^{19} photons/s mm^2. The fluorescence emission spectrum was recorded using a CCD-matrix array with attached polychromator (InstaSpec IV) with a spectral resolution of 1 nm or better.

2.2.2. Picosecond time-resolved fluorescence measurements

Measurements were performed at an excitation wavelength of 570 nm using the output of a cavity-dumped dye laser (Coherent 701-2CD), pumped by a Nd:YAG laser (Coherent Antares). Without saturable absorber jet, the achieved pulse had a duration of 10 ps at a repetition rate of 3.8 MHz. The excitation intensity for these high

intensity experiments was ~70 nJ/mm^2 pulse. This corresponds to a photon flux density of about 2.1×10^{11} photons/mm^2 pulse, an average photon flux of 7.8×10^{17} photons/mm^2 s and a peak photon flux of 2.1×10^{22} photons/mm^2 s. For measurements at low light intensity, attenuation was achieved by a combination of $\lambda/2$ plate and a polarizer to 2 nJ/mm^2 and, consequently, photon fluxes lower by a factor of 35. For detection of fluorescence kinetics, a time-correlated single-photon counting setup (TCSPC) was used, providing an instrument response function of 25.0 ps [11]. All data were measured under magic angle conditions. Using standard deconvolution procedures averaged lifetimes carry an approximate error of <20%.

2.2.3. Femtosecond transient absorption measurements

Transient absorption measurements were performed using a Ti:Sapphire oscillator/regenerative amplifier system which has been described in detail elsewhere [43]. Briefly, the output at 780 nm of an Ar^+-laser pumped commercial Ti:Sapphire oscillator (MIRA/Coherent, repetition rate 76 MHz, pulse width 100 fs) was temporarily broadened to 150 ps before seeding a regenerative amplifier system (BMI Alpha 1000S) pumped at 10 W by a Nd:YLF laser (BMI 621D) at 526 nm. The amplified pulses (1.4 mJ) were split into pump and probe beam (9:1). After separate recompression optical pulses at 780 nm with a pulse duration of 120 fs were obtained. The more intense pulses were frequency-doubled and directed through an OPG/OPA setup to produce a signal wave tunable from 450 to 700 nm for excitation. The weaker probing pulses were sent to a variable delay line four times allowing a total delay between pump and probe pulses of 5 ns with increments of 33 fs before they were focused in a 2 mm sapphire crystal to produce a white light continuum. By means of a chirp-compensated, stepper motor controlled spectrometer, a spectral region with a bandwidth of 12 nm was selected from this continuum. The relative polarization between pump and probe beam were set to the magic angle to avoid rotational depolarization effects. Pump and probe beams were focused under an angle of 8° at a 2 mm fused silica cuvette containing the sample. The pulse duration was 130 fs at a repetition rate of 0.5 kHz for the excitation pulse. The average peak power was 20 μJ/mm^2 pulse. This corresponds to photon flux densities of 5.9×10^{13} photons/mm^2 pulse, an average photon flux of 3.0×10^{16} photons/mm^2 s and a peak photon flux of 4.6×10^{26} photons/mm^2 s during the excitation pulse. Comparison of excitation conditions is given in Table 1.

Table 1
Excitation conditions in the different types of experiments

Excitation source	Photon flux density (photons/mm^2 s)	
	Averaged	Peak
cw ($\lambda_{exc} = 514$ nm)	1×10^{17} to 3×10^{19}	
TCSPC (3.8 MHz, $\lambda_{exc} = 570$ nm) (low intensity)	2.2×10^{16}	6.0×10^{20}
TCSPC (3.8 MHz, $\lambda_{exc} = 570$ nm) (high intensity)	7.8×10^{17}	2.1×10^{22}
fs absorption (0.5 kHz, $\lambda_{exc} = 565$ nm)	3.0×10^{16}	4.6×10^{26}

3. Results

3.1. Steady-state spectroscopy at low and high light intensities

Wt-asFP595. As shown in Fig. 1, the absorption spectra show vibronic structure and a red-shift of 9 nm upon cooling to 150 K, which is further red-shifted upon long-term illumination. The maximum of the fluorescence excitation spectra coincides well with the one of the absorption spectra in Fig. 1(a) and (b). Broadening of the excitation spectra is caused by the decreased spectral resolution due to the wide entrance/exit slits of the monochromators necessary to meet the conditions of the extremely low

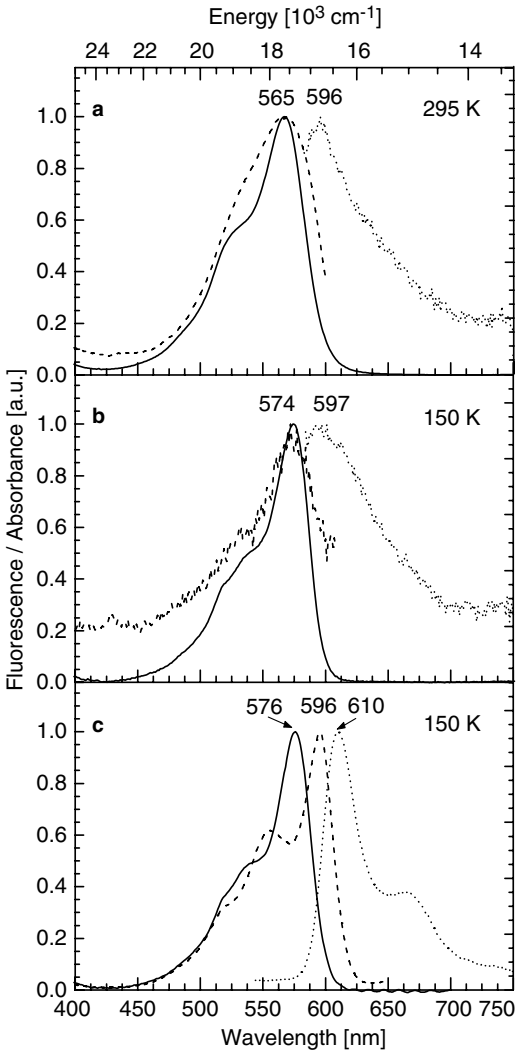

Fig. 1. *wt-asFP595*. Absorption (—), fluorescence (···, $\lambda_{exc} = 560$ nm) and fluorescence excitation (---, $\lambda_{det} = 675$ nm); (a) and (b) dark protein; (c) after 15 h illumination at 560 nm, 14 μW/mm^2.

fluorescence quantum yield. From the absorption and fluorescence maxima the upper limit of the Stokes shift is estimated to be in the range of 800–1000 cm^{-1} and therefore slightly smaller than the Stokes shift of the anionic state $(RO^-)^*$ in GFP (1280 cm^{-1}) [11]. A Stokes shift in this range provides a strong argument against the protonated neutral state ROH contributing as a majority to the absorption spectrum. This small Stokes shift can neither account for excited state proton transfer, which in GFP leads to an apparent Stokes shift of ~5600 cm^{-1}, nor for the emission from (ROH)* for which the Stokes shift in wt-GFP and Tyr66 mutants still amounts to ~3000 cm^{-1} [11,14]. Thus, on the basis of exclusion, we attribute the dark species in the chromoprotein asFP595 to either the anionic or the zwitterionic state.

Long-term low intensity irradiation at room temperature does not lead to an increase of fluorescence, not even upon immobilizing the chromoprotein asFP595 in a PVA matrix in order to suppress diffusional escape of kindled protein. However, at low temperature (e.g., at 150 K as in Fig. 1(c)) it was easily possible to increase the fluorescence quantum yield of the chromoprotein by about a factor of 20. Upon long-term, low-intensity treatment, fluorescence and fluorescence excitation spectra are red-shifted. Due to the increase in fluorescence quantum yield, it was possible to resolve two minor peaks indicating a vibronic progression of ~1300 cm^{-1}, similar to the one observed in GFP [11]. The fluorescence excitation spectrum is identical with the absorption spectrum of the fluorescing minority, while the predominant absorber is still the dark state.

High intensity illumination using a cw Ar^+-laser leads to fluorescence kindling already at room temperature. The observed red-shift of the fluorescence maximum (~3 nm, Fig. 2(a)) is in agreement with the low temperature, low intensity experiments (Fig. 1(b) and (c)). We note in passing, that in the fluorescent protein dsRed, the steady-state fluorescence spectrum continuously shifts to the red with increasing light intensity implying excitation-driven conformational rearrangements also in this case [44]. However, in the context of the kindling mechanism, the most relevant observation, which is not reported for dsRed, is the increase of the fluorescence quantum yield with increasing excitation intensity (Fig. 2(b)), leveling off at high intensities.

The mutant asFP595–Ala148Ser. Qualitatively, the steady-state absorption and fluorescence spectra at room temperature (Fig. 3(a)) resemble the corresponding spectra of wt-asFP595. In contrast to wt-asFP595, the fluorescence excitation spectrum is significantly red-shifted as compared to the absorption spectrum. This deviation indicates that the majority population is non-fluorescent, while a minority red-shifted absorption is responsible for the steady-state emission which is by about a factor of 10 higher than in wt-asFP595. Upon cooling to 150 K (i.e., below the glass point), the absorption maximum shifts towards the red and coincides now with the maximum of the excitation

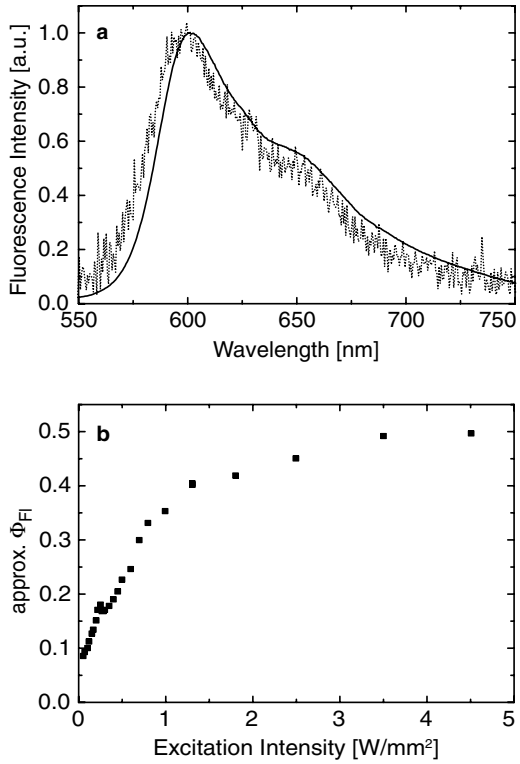

Fig. 2. *wt-asFP595*. Fluorescence kindling by high intensity illumination at $\lambda_{exc} = 514$ nm (cw Ar^+-laser). (a) Steady-state fluorescence spectrum measured at different excitation intensities: 0.04 W/mm^2 (···) and 10.5 W/mm^2 (—); (b) fluorescence quantum yield versus excitation intensity, absolute numbers based on comparison to GFP (see text).

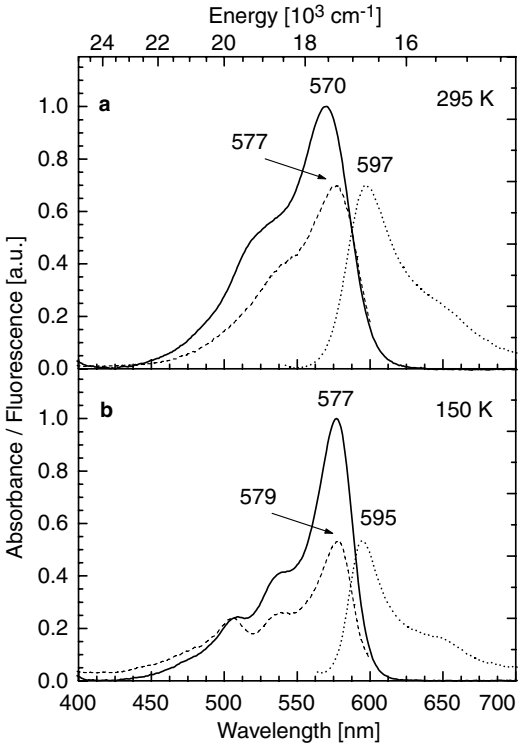

Fig. 3. *asFP595–Ala148Ser mutant*. Steady-state spectra under low light intensity conditions at 295 and 150 K. Absorption (—), fluorescence (···, $\lambda_{exc} = 540$ nm) and fluorescence excitation (---, $\lambda_{det} = 650$ nm).

spectrum, which is not affected by the low temperature (Fig. 3(b)). This observation is made even in the absence of high light intensity. It shows that the dark and fluorescent species are in a temperature dependent equilibrium favoring the latter one at low temperatures. With respect to the Stokes shift at low temperature, the mutant (excited with low light intensity) and wt-asFP595 (excited with high intensity illumination) exhibit similar behavior, except a slight blue-shift of the absorption and emission spectra of the mutant. Unexpectedly, neither at low nor at high light intensities an appreciable absorption in the blue (peaking at 450 nm) is observed, which has been reported for wt-asFP595 to revert the kindling effect [34], although the contribution of the fluorescent state in this mutant is much higher than in the wild type mother protein.

3.2. Femtosecond to picosecond time-resolved spectroscopy

The fluorescence lifetime profile after excitation with ps pulses (FWHM 10 ps) depends on the excitation intensity. At low (~2 nJ/mm^2 pulse) and high excitation (~70 nJ/mm^2 pulse) intensities, the fluorescence decayed non-exponentially with three time constants (Fig. 4):

low intensity TCSPC:

$\tau_1 = 17$ ps (84%),

$\tau_2 = 230$ ps (11%),

$\tau_3 = 1.6$ ns (5%);

high intensity TCSPC:

$\tau_1 = 150$ ps (45%),

$\tau_2 = 800$ ps (30%),

$\tau_3 = 2.2$ ns (25%).

From these results it is obvious, that high intensity illumination leads to an increase of the amplitudes of the long time components at intensities (averaged over the pulse train) which are comparable to the photon flux, where the cw experiment (Fig. 2) showed an intensity dependence of the fluorescence quantum yield. Based on this observation, the fluorescence kindling effect seems to be intimately related to a species with a lifetime of the excited state in the ns regime. As the TCSPC setup is insensitive to decay dynamics shorter than 25 ps (FWHM of the instrument response function), the short time component of 17 ps observed at low light intensity is only indicative of a fast process beyond resolution.

The superlinear dependence of fluorescence intensity on the excitation intensity, as observed under cw conditions, requires a process, where at least more than one exciting photon is involved. In order to test whether these photons are absorbed simultaneously or sequentially, and to time-resolve the excited state dynamics, fs pump/probe experiments have been performed (Fig. 5). Although the peak photon flux densities during the excitation pulse are higher by more than a factor of 10^4 as compared to the above mentioned high intensity TCSPC measurements, the ratio of the averaged intensities is reversed. Similar to the fluorescence experiments, also in fs absorption non-exponential kinetics are observed. Probing the decay of the excited state via stimulated emission at a wavelength close to the steady-state fluorescence maximum and the ground state recovery in the blue wing of the absorption spectrum, the resulting time traces exhibit similar temporal evolution. Simultaneously fitting both traces the following time constants (and relative amplitudes) are obtained:

$\tau_1 = 320$ fs (78%),

$\tau_2 = 2.6$ ps (19%),

$\tau_3 = 12.1$ ps (3%).

Obviously, the predominant decay component (320 fs) of the excited state is ultrafast. Since the recovery of the ground state follows similar kinetics with respect to components and amplitudes, the decay process of the excited state is assigned to internal conversion. Detailed studies on the relative contributions of structural heterogeneity and vibrational cooling to the ps components are in progress.

The lack of a ns component in this fs absorption experiment indicates that the fluorescent species obviously could not be populated under these conditions of an ultrahigh

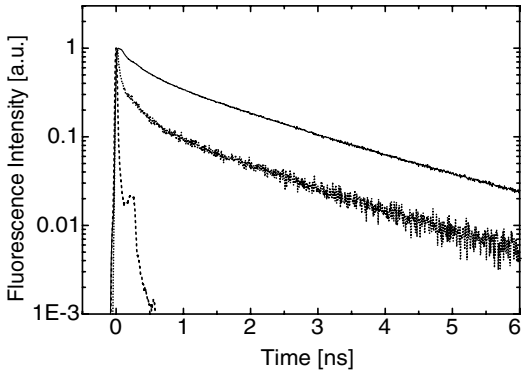

Fig. 4. *wt-asFP595*. Fluorescence decay traces at 298 K ($\lambda_{exc} = 570$ nm, $\lambda_{det} = 595$ nm); excitation at high (70 nJ/mm^2 pulse, —) and low intensity (2 nJ/mm^2 pulse, ···); IRF: 27 ps (---).

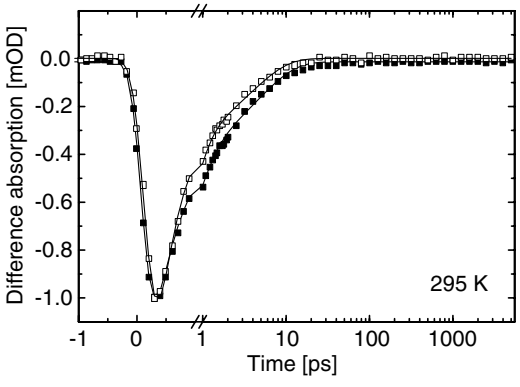

Fig. 5. *wt-asFP595*. Temporal evolution of stimulated emission probed at 590 nm (□), and ground state recovery probed at 550 nm (■); $\lambda_{exc} = 565$ nm, pulse duration and energy: 130 fs and 20 μJ/mm^2 pulse, IRF: 200 fs.

peak photon flux. As these conditions would clearly favor simultaneous absorption of two photons and no indication for a species with a long fluorescence lifetime could be found, the kindling mechanism must be based on sequential absorption of two photons within a time window significantly longer than the fs excitation pulse, i.e., $\gg$150 fs. In contrast to high intensity cw excitation, no increase of fluorescence intensity could be observed in the fs absorption experiment. This can be due to population of the kindled state below the sensitivity of the transient absorption experiment ($\leqslant$5%). In fact, this is expected, as the average photon flux is about 100 times lower than under the conditions of high intensity cw excitation.

Time traces of the mutant Ala148Ser (analogous to those of wild type in Fig. 5) are also multiexponential and can be globally fitted to

$\tau_1 = 243$ fs (56%),
$\tau_2 = 52$ ps (13%),
$\tau_3 = 386$ ps (13%),
$\tau_4 = 2.4$ ns (18%).

These kinetic data are consistent with the notion that also in the mutant ultrafast internal conversion is the predominant radiationless process in accordance with the discrepancy between steady-state absorption and fluorescence excitation spectra (Fig. 3(a)). The relative amplitude of the shortest time component is smaller than in wild type asFP595, while time constants and amplitudes of long components are relatively large. Thus, in the mutant significant contributions to the fluorescence originate from the fluorescent species already present in thermal equilibrium.

The most relevant spectroscopic and kinetic characteristics of the fluorescence kindling phenomenon underlying the kinetic scheme of Fig. 6 are summarized as follows:

1. The small Stokes shift of the initial dark state of $\approx$1000 cm^{-1} excludes a neutral chromophore. Provided that the analogy to wt-GFP holds, the most probable states for the dark chromophore are the zwitterion or the anion.

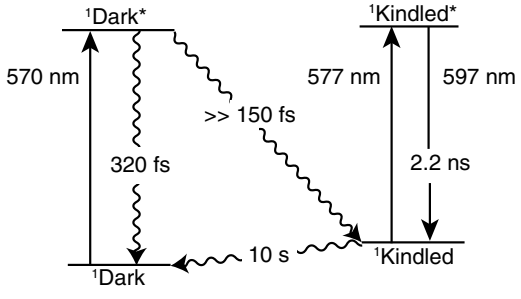

Fig. 6. *Kinetic scheme (295 K)*. Depending on the predominant kindling mechanism, the dark non-planar *trans* isomer is either the zwitterion (O^-, NH^+) or the anion (O^-, N). The kindled state is a planar anion independent of the initial dark state. Maxima of absorption and fluorescence are given for the mutant asFP595–Ala148Ser since the analogous data set for 295 K is not available for wt-asFP595.

2. The low fluorescence quantum yield ($\Phi_{Fl} \leqslant 10^{-4}$) of asFP595 is reflected in a large amplitude ($\approx$80%) of the shortest lifetime ($\sim$320 fs) of the excited dark state. Since ground state recovery occurs on the same time scale, the predominant radiationless deactivation channel of the excited state is assigned to internal conversion.
3. Kindling of fluorescence depends on the sequential absorption with a delay exceeding by far the width of the fs excitation pulse ($\gg$150 fs).
4. The fluorescent species shows a characteristic red-shift of $\sim$20 nm in absorption and emission as compared to the initial dark state and a fluorescence lifetime of 2.2 ns. With the experimental setup used in this work, the red-shift is observed only at low temperature due to the increased efficiency in pumping the fluorescent species.

4. Quantum-mechanical calculations of different protonation states

In order to obtain some spectroscopic guidelines on the potential involvement of different protonation states of the chromophore in the photophysics of asFP595, quantum-chemical calculations were performed on the basis of the recent X-ray structural data [36,38]. Both structures relate to the chromoprotein KFP that is a mutant of asFP595 carrying the key mutation Ala148Gly (numbering in accordance to GFP). Throughout this paper, we tacitly assume that the principal features of the chromophore and its environment are similar for both proteins, wt-asFP595 and its mutant KFP.

As we did in a previous study [33], the INDO/S method was employed for the calculation of spectroscopic parameters of the different protonation states of the two chromophores, while the geometry optimization was carried out within the DFT/B3LYP method. The DFT calculations were performed with the program Gaussian 98 [45] using the standard basis set 6-31 G. Similar spectroscopic parameters were also obtained within the NDDO/G method.

Considering the neutral chromophore (HO, N), its anion (O^-, N), the zwitterion (O^-, NH^+), and the cation (HO, NH^+), calculations showed that the neutral and cationic forms can be neglected as states determining the photophysics of asFP595 because of the remarkably (0.6–1.0 eV) higher absorption energies as compared to the experimental maximum at 565 nm for the dark state (Fig. 1). Then, with respect to the kindling mechanism we

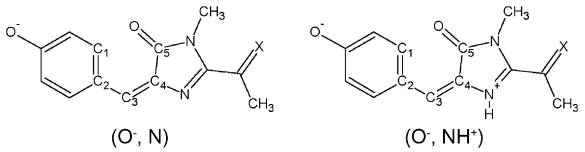

Scheme 1. Anionic (O^-, N) and zwitterionic (O^-, NH^+) forms of the two chromophore structures A and B with X = NH (A) [36] and X = O (B) [38].

are focusing on the anionic and the zwitterionic forms of the chromophore. One of the most intriguing features of the two chromophore structures A and B is the distortion of the chromophore from planarity. In structure A, the dihedral angles $\angle C_1$–C_2–C_3–C_4 (rotation about C_2–C_3 bond) and the angle $\angle C_2$–C_3–C_4–C_5 (rotation about C_3–C_4 bond) are 31.1° and −21.1°, respectively. Regarding structure B, the distortion is remarkably smaller with dihedral angles of only 8.1° and 0.6°.

In view of the highly distorted structure A, it is of interest to estimate also the effect of this deviation from planarity on the absorption energies of the relevant protonation states, the anion and zwitterion. With this goal in mind, a partial and full geometry optimization has been performed. B3LYP calculations show that the deformation energy of the *trans* anion is 24 kJ/mol. This value defines the total energy difference between two chromophore conformations, one partially optimized with both dihedral angles fixed and the other one fully optimized and planar. Assuming that the distorted structure is close to the reaction path of the excited state decay, a dramatic increase of the decay rate is expected due to the resulting small energy gap between the excited state and the ground state. Since *trans–cis* isomerization may be involved in internal conversion, the excitation energies of the corresponding *cis* isomers were also calculated (Table 2).

From the data given in Table 2 the following conclusions are drawn:

1. The replacement of the imino group in structure A by a carbonyl in structure B does hardly affect the spectroscopic properties of the chromophore.
2. The large distortion of the chromophore structure A [36] is not influencing the absorption energies of either anion or zwitterion by more than 0.1 eV.
3. The dark species cannot be assigned to either anion or zwitterion since, in these calculations, local interactions between the chromophore and its contacts to nearby amino acid residues are neglected. The limitations of such calculations based on the isolated chromophore are illustrated using GFP as an example [46]. For instance, electrostatic contacts of the anion with Water1, Tyr145, His148, Thr65 result in a blue-shift of absorption by 0.1 eV, while a red-shift of 0.1 eV is caused by interactions of the chromophore with Arg96 and Gln94. Due to these compensating effects, the dependence of the chromophore's absorption energy on local interactions with amino acid residues in the binding pocket turns out to be weak. For instance, for the isolated anion of the GFP chromophore DFT calculations yield an absorption energy of 1.81 eV as compared to 1.82 eV in the presence of Arg96, Gln94, W1, Tyr145, His148, Thr65 [46]. However, while in GFP the total effect seems to be negligibly small, interaction of the chromophore with individual amino acid side chains can lead to remarkable changes in the absorption spectra. Following this line of arguments, relaxation of the protein matrix and/or change of conformation of the chromophore (e.g., *trans–cis* isomerization) may be followed by appreciable variations (∼0.1 eV) of excitation energies falling into the overall span of 0.2 eV given in Table 2.

Table 2
Calculated oscillator strengths (F) and absorption energies (eV) for the non-planar and planar anion and zwitterion in their *trans* and *cis* conformations based on structure A [36]

Protonation state of the chromophore	F	$h\nu$ (eV)	λ (nm)
trans-Anion (O^-, N) non-planar	1.33	2.30	540
trans-Anion (O^-, N) planar	1.41 (1.38)	2.43 (2.44)	511 (507)
cis-Anion (O^-, N) planar	1.22 (1.20)	2.39 (2.41)	519 (515)
trans-Zwitterion (O^-, NH^+) non-planar	1.37	2.26	548
trans-Zwitterion (O^-, NH^+) planar	1.35 (1.37)	2.29 (2.23)	541 (536)
cis-Zwitterion (O^-, NH^+) planar	1.14 (1.02)	2.20 (2.24)	562 (553)

The respective values for the more recent structure B [38] are given in parenthesis. In view of the small effects on the spectroscopic parameters caused by the large deviation from planarity in structure A, the respective values for the non-planar structure B are not given since they hardly differ from the ones of the respective planar states.

5. Ultrafast internal conversion and mechanisms of kindling

The chromophore in its initial dark state is either an anion or a zwitterion. This assignment is based on the steady-state spectra and supported by quantum-chemical calculations of the absorption energies of the different protonation states. According to the X-ray structures [36,38], the photophysical processes take off from a nonplanar *trans*-form of the dark chromophore showing an absorption maximum at 565 nm with an extinction coefficient of $1.5 \times 10^5\ M^{-1}\ cm^{-1}$ [40]. Its fluorescence is peaking at 595 nm and decaying within 320 fs. A comparison of a lifetime of 320 fs for the excited dark state to a lifetime of the 2.2 ns for the photoconverted fluorescent state limits the fluorescence quantum yield of the dark state to $\Phi_{Fl} \leqslant 10^{-4}$, in agreement with the limit $\Phi_{Fl} < 0.001$ given on the basis of steady-state measurements [33].

In principle, the predominant contribution to a radiationless decay within 320 fs may be any cyclic process, which recovers the electronic ground state on an ultrashort time scale. In case electron or proton transfer reactions would prevail, the measured 320 fs would correspond to the rate-determining step, i.e., the back reaction has to be even faster. Assuming such a short-lived intermediate to be improbable, fast internal conversion is attributed to be the predominant radiationless pathway of the excited dark state.

Independent of the nature of the initial dark state, zwitterion or anion, conformations of the chromophore that

are twisted away from planarity around the bridging —CH= group are expected to enhance internal conversion. This enhancement is caused by the decrease of the energy gap between S_1 and S_0 potential energy surfaces [27,28] near a conical intersection, which favors a transition to the electronic ground state.

As indicated in the kinetic scheme of Fig. 6, a low quantum yield leakage process on a time scale significantly longer than 150 fs leads to fluorescence kindling. At rates considerably smaller than the one of internal conversion, a species is formed which, upon excitation by a second photon, decays with a fluorescence lifetime of 2.2 ns (Fig. 4). Alternatively, this photoconverted ground state species may return thermally to the initial dark state on the time scale of 10 s [33,34]. In contrast to wt-asFP595 where, at low light intensities, the equilibrium between the dark and fluorescent state rests heavily on the dark state, this is much less the case in the mutant Ala148Ser, where the equilibrium is shifted to the fluorescent state.

In the attempt to explain the kindling mechanism, we present two exemplary scenarios (i) and (ii), differing in the extent to which *trans–cis* isomerization contributes to the formation of the fluorescent state. In scenario (i), the native dark state is a zwitterion, in scenario (ii), it is an anion, but in a more complex scheme, this scenario would also apply to a zwitterion.

5.1. Kindling in the absence of trans–cis isomerization

The structural features highlighted in Fig. 7 are particularly relevant for this scenario, since it involves a zwitterion, present either in the dark ground state or formed upon excitation of a dark anionic state. We mention in passing that these structural details are invariant in the two X-ray structures [36,38]. Short distances between tyrosyl oxygen, a nearby Ser158 and a water molecule favor stabilization of the deprotonated tyrosyl group due to strong hydrogen bonding. Another strong hydrogen bond (2.73 Å [36], 2.7 Å [38]) between the nitrogen atom of the imidazolinone ring and Glu215 facilitates proton transfer between these sites while an electrostatic contact of oxygen with Arg92 (2.92 Å [36], 2.8 Å [38]) stabilizes the negative charge on the carbonyl oxygen. Thus, on the basis of this hydrogen bond network, the chromophore in its dark state may exist already in its zwitterionic form.

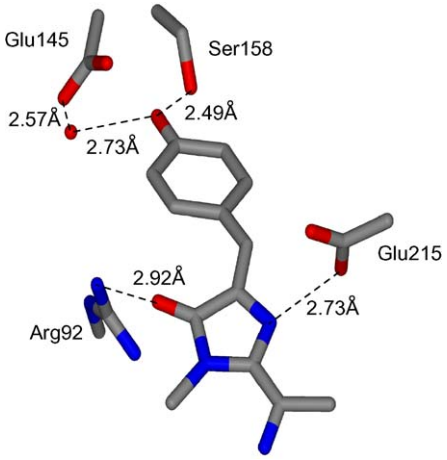

Fig. 7. *The KFP chromophore*. Its hydrogen bond contacts in the protein binding site using the coordinates given by the X-ray structure [36].

Computational modeling of GFP indicates that the zwitterion may also be present in wt-GFP [47]. In particular, upon excitation the zwitterion gains stability as compared to the other protonation states. On the basis of the estimated microscopic constants for the equilibrium of neutral and zwitterion states, it was concluded that in GFP the zwitterion is not populated in the electronic ground state. However, in asFP595 changes of both, the structure of the chromophore and its protein environment, may stabilize the zwitterion already in its electronic ground state. Since among the different protonation states, the zwitterion displays the smallest energy gap between the S_1 and S_0 potential energy surfaces [27,28] near a conical intersection [32], efficient internal conversion is favored. Besides the *a priori* favorable electronic potential energy surfaces, conformations of the chromophore that are twisted away from planarity around the bridging —CH= group are expected to further enhance internal conversion.

A crucial requirement for this mechanism to work is that upon excitation ($S_0 \rightarrow S_1$) of the dark state, a considerable redistribution of the charge density occurs. In fact, this is expected since a major component of the large dipole moment change of the zwitterion of $\Delta\mu = 11.4$ D is due to intramolecular charge transfer from the tyrosyl to the imidazolinone ring. For comparison, the analogous dipole moment change of the zwitterion in GFP ($\Delta\mu = 5.23$ D) is much smaller. As a consequence of the drastic change in electrostatics upon excitation of the dark chromophore, its protein environment will relax towards a structure, which has responded to the increase of negative charge density at the heterocyclic nitrogen. In particular, one may expect that the hydrogen bond between the imidazolinone ring of the chromophore to Glu215 (Fig. 7) will become weaker. Then, following the decay of the excited, conformationally relaxed state by internal conversion, the zwitterion finds itself in the electronic ground state, although in a non-equilibrium environment. In this situation the zwitterion will be destabilized and may recover the non-planar dark state by slow protein relaxation on the time scale of 10 s. As an alternative to this dark state recovery, and most relevant for the kindling mechanism (Fig. 6), the conformationally relaxed zwitterion may undergo deprotonation of the heterocyclic nitrogen. Thereby it may form a metastable planar anion maintaining the *trans* conformation of the initial dark state. This planar anion may absorb a second photon and, since internal conversion in the anion's singlet state is by far less favored as compared to the zwitterion, fluorescence is drastically enhanced. Its decay time of 2.2 ns is now similar to one of the excited anion in GFP (3.3 ns). On the basis of these lifetimes, the fluorescence quantum yield of the kindled

fluorescent state is $\Phi_{Fl} = 0.5$, if based on $\Phi_{Fl} = 0.8$ for wt-GFP [4]. Together with the time constant of 320 fs for internal conversion, the fluorescence quantum yield of asFP595 in its dark state is as low as $\Phi_{Fl} = 7 \times 10^{-5}$.

Scenario (i) has to be invoked in case the future X-ray structure of asFP595, or an analogue mutant like KFP, in the photoconverted state would still show the chromophore in its trans conformation.

5.2. Kindling induced by isomerization of a non-planar trans-anion to a planar cis-anion

In the simplest version of this scenario, the dark state is assumed to be an anion. As mentioned above, also in the anionic state the non-planar structure of the chromophore is expected to favor fast internal conversion. This expectation is supported by the result that already small torsional deformations of the Tyr66-C bond in GFP are sufficient to cause internal conversion [30]. In addition, a relatively open protein pocket, partially due to main chain cleavage, may enhance rotational motion around the exocyclic bonds with a low activation barrier. However, even in the tighter GFP binding cleft, space requirements for chromophore isomerization seem to be met [17]. We note in passing, that the involvement of the hula-twist deformation in the fluorescence decay can be excluded due to the ultrashort lifetime of the excited dark state. This failure of hula-twist motion has been proposed on the basis of its high activation energy resulting from a recent quantum-chemical study of the isolated GFP-chromophore [30].

Competing with ultrafast internal conversion of the excited *trans* isomer, a low quantum yield transition to the *cis* isomer may occur. In the simplest case, this mechanism is represented by the kinetic scheme of Fig. 6, if the dark and the fluorescent states are identified with *trans* and *cis* isomers of the anion, respectively. Such a kindling mechanism is also the key process in the interesting hypothesis that *trans–cis* isomerization is facilitated by a conformational switch involving the side chain of His197 [38]. In the special case of asFP595 and possibly also of other non-fluorescent proteins, the activation barrier for rotational motion in the excited *cis*-isomer is expected to be higher than that of the *trans*-isomer. This difference in the activation barrier results from the interaction of the chromophore with the protein matrix demanding for a non-planar structure of the *trans* isomer.

Another important parameter of such a mechanism is the activation barrier of the back transformation of the *cis* isomer in its ground state to the dark *trans* isomer. This activation barrier determined experimentally to be 71 kJ/mol [38] is expected to be sufficiently low to restore the initial *trans*-chromophore within the experimental time windows of 10 and 100 s for wt-asFP595 and its Ala148Gly mutant (i.e., KFP), respectively. We note that this activation barrier in the protein is close to the one (55 kJ/mol) determined by NMR spectroscopy for a model GFP chromophore in solution [48]. These NMR experiments showed that *cis–trans* isomerization is almost independent of the protonation state and that the respective activation energies are much lower than the ones predicted by quantum-chemical calculations [26–28].

5.3. Kindling at low temperatures

At 295 K, fast internal conversion gives rise to a rapid depopulation of the excited singlet state and the efficiency of competing photoconversion is small. In order to detect kindled fluorescence, photoconverted chromophores have to be excited by a second photon. The excitation probability depends on the lifetime of the photoconverted state and, thus, on the time constant of conformational back relaxation to the initial dark state. The observation that at low temperature, even after long-term illumination with green light, no measurable effect on the absorption spectrum of wt-asFPF595 is observed, allows us to conclude, that fast internal conversion of the excited dark state is still the dominating radiationless decay process, although the accumulation of the fluorescent state is strongly favored. Interestingly, upon lowering the temperature to 80 K, the formation of the fluorescent state is less efficient than at 150 K indicating that the photoconversion process itself is thermally activated.

5.4. Blue light quenching of the fluorescent state

The reported blue light reversal of the fluorescence kindling effect [33–35], which in any mechanism should be associated with the removal of the planar anion, is reported to be initiated by illumination at wavelengths around 450 nm. Since so far, detailed experiments are missing, the nature of the state excited at 450 nm is unknown. For instance, in analogy to the parent protein GFP, this state may be a neutral chromophore in equilibrium with its anionic form [38], or, alternatively, the higher $S_1 \rightarrow S_2$ excited state of the anion. Calculations indicate that the oscillator strength of the $S_0 \rightarrow S_2$ transition is rather small, i.e., by a factor of $\sim 10^3$ smaller than for the $S_0 \rightarrow S_1$ transition. The proton affinity of the heterocyclic nitrogen of the imidazolinone ring increases with the extent of electronic charge being transferred from the tyrosyl [26]. Analysis of intra-chromophore charge transfer in the S_1 excited state of the anion indicates that in both isomers 0.30 electrons are shifted from the tyrosyl ring to the heterocycle, while in the S_2 excited state 0.6 and 0.7 electrons are transferred in the *trans* and *cis* isomers, respectively. In scenario (i) this increase of charge transfer would favor the formation of the zwitterion, which may finally relax to the initial dark state.

6. Concluding remarks

The overarching feature of the non-fluorescent protein asFP595 is the ultrafast (320 fs) internal conversion ($S_1 \rightarrow S_0$) of the excited chromophore in its *trans* conformation. The initial dark state may be either a zwitterion

or an anion. Based on quantum chemical arguments, internal conversion is supported by the non-planarity of the chromophore. Due to the proximity of the S_1 and S_0 potential energy surfaces, such an enhancement is expected to be strongest for the zwitterion.

A qualitative correlation [49] between fluorescence lifetime and chromophore conformation has been extracted from fluorescence lifetime data and the X-ray structures of two other coral proteins, Rtms5 [50] and eqFP611 [51]. Both proteins exhibit the well-known 11-stranded β-can structure and carry the respective chromophores in *trans* conformation. As in asFP595, the tyrosyl ring in the Rtms5 chromophore is non-planar and at the same time this protein is non-fluorescent ($\Phi_{Fl} < 0.001$). In contrast, the chromophore of the eqFP611 protein shows a fluorescence lifetime of 2.5 ns and a fluorescence quantum yield of $\Phi_{Fl} = 0.45$ [52]. In this fluorescent protein, the chromophore adopts a planar conformation with the tyrosyl group sandwiched between His197 and Phe174. As this stacking ensures the coplanarity of the tyrosyl residue and the imidazolinone ring, coplanarity of the chromophore seems to be crucial for high fluorescence quantum yield. In eqFP611 the sandwiched tyrosyl group has restricted motional freedom keeping the chromophore in the coplanar conformation, whereas in Rtms5, the guanidium group of Arg197 seems to prevent a coplanar structure of the chromophore. In a detailed discussion [38] of the structural basis relevant for fluorescence kindling of the asFP595 analogue KFP, the key feature setting the scene turns out to be the distortion of the chromophore from planarity. There are convincing arguments that this feature overrules any specific role of the initial isomer (*trans* or *cis*) as well as the increased mobility of the chromophore due to its partial detachment from the polypeptide backbone.

Let us finally comment on the observation that the fluorescence quantum yield of the protein-bound KFP chromophore is by a factor of 10 smaller than the one of the KFP chromophore free in non-viscous solution [40]. Such a surprising discrepancy in the internal conversion rates may be rooted in the specific interactions between the chromophore and its protein environment responsible for both, its distortion from planar conformation and its protonation state, anion or zwitterion. Non-planarity is expected to affect the electronic potential energy surfaces of ground and excited states in such a way, that efficient internal conversion is achieved since the excited non-planar chromophore needs less nuclear motion to cross from the S_1 over to the S_0 surface as compared to its planar state. Therefore, in the protein cleft, the activation energy of internal conversion is expected to be small enough to compensate for a restriction of the chromophore's internal flexibility as compared to non-viscous solution.

Although, at this stage of evidence, the nature of the fluorescence kindling mechanism is still speculative, this problem is expected to be solved by a future X-ray structure of a non-fluorescent protein in its photoconverted state. Structural information will also decide on the relevance of the conformational switch [38] based on His197, which has been proposed for stabilization of different isomers. Apart from a basic interest in protein-controlled photoconversion and its potential implications in biotechnology, ultrafast degradation of excitation energy in a light-exposed protein may bear biological significance, since short lifetimes of excited states optimize the photochemical stability of a heavily colored organism.

Acknowledgments

We are indebted to Professor Beate Röder and her group at the Humboldt University in Berlin for letting us perform steady-state high intensity experiments. A.P.S. and K.A.L. are grateful for financial support in the frame of the Program "Molecular and Cellular Biology" of the Russian Academy of Sciences. Financial support from the Deutsche Forschungsgemeinschaft (SFB 533) is gratefully acknowledged.

References

[1] R.Y. Tsien, Annu. Rev. Biochem. 67 (1998) 509.
[2] M. Zimmer, Chem. Rev. 102 (2002) 759.
[3] M. Chalfie, Y. Tu, G. Euskerchen, W.W. Ward, D. Prasher, Science 261 (1994) 802.
[4] H. Morise, O. Shimomura, F.H. Johnson, J. Winant, Biochemistry 13 (1974) 2656.
[5] F. Yang, L.G. Moss, G.N. Phillips, Nat. Biotechnol. 14 (1996) 1246.
[6] M. Ormö, A.B. Cubitt, K. Kallio, L.A. Gross, R.Y. Tsien, S.J. Remington, Science 273 (1996) 1392.
[7] R. Heim, D.C. Prasher, R.Y. Tsien, Proc. Natl. Acad. Sci. USA 91 (1994) 12501.
[8] A.B. Cubitt, R. Heim, S.R. Adams, A.E. Boyd, L.A. Gross, R.Y. Tsien, TIBS 20 (1995) 448.
[9] B.G. Reid, G.C. Flynn, Biochemistry 36 (1997) 6786.
[10] M. Chattoraj, B.A. King, G.U. Bublitz, S.G. Boxer, Proc. Natl. Acad. Sci. USA 93 (1996) 8362.
[11] H. Lossau, A. Kummer, R. Heinecke, F. Pöllinger-Dammer, C. Kompa, G. Bieser, T. Jonsson, C. Silva, M. Yang, D. Youvan, M.E. Michel-Beyerle, Chem. Phys. 213 (1996) 1.
[12] A. Kummer, C. Kompa, H. Lossau, F. Pöllinger-Dammer, M.E. Michel-Beyerle, C. Silva, E. Bylina, W. Coleman, M. Young, D. Youvan, Chem. Phys. 237 (1998) 183.
[13] A. Kummer, J. Wiehler, H. Rehaber, C. Kompa, B. Steipe, M.E. Michel-Beyerle, J. Phys. Chem. B 104 (2000) 4791.
[14] A.D. Kummer, J. Wiehler, T.A. Schüttrigkeit, B.W. Berger, B. Steipe, M.E. Michel-Beyerle, ChemBiochem 3 (2002) 359.
[15] A. Kummer, C. Kompa, H. Niwa, T. Hirano, S. Kojima, M.E. Michel-Beyerle, J. Phys. Chem. B 106 (2002) 7554.
[16] D. Mandal, T. Tahara, N.M. Webber, S.R. Meech, Chem. Phys. Lett. 358 (2002) 495.
[17] N.Y.A. Baffour-Awuah, M. Zimmer, Chem. Phys. 303 (2004) 7.
[18] R.M. Dickson, A.B. Cubitt, R.Y. Tsien, W.E. Moerner, Nature 388 (1997) 355.
[19] U. Haupts, S. Maiti, P. Schwille, W.W. Webb, Proc. Natl. Acad. Sci. USA 95 (1998) 13573.
[20] B. Lounis, J. Deich, F.I. Rosell, S.G. Boxer, W.E. Moerner, J. Phys. Chem. B 105 (2001) 5048.
[21] E.J. Peterman, S. Brasselet, W.E. Moerner, J. Phys. Chem. A 103 (1999) 10553.
[22] M.F. Garcia-Parajo, G.M.J. Segers-Nolten, J.-A. Veerman, J. Greve, N.F. van Hulst, Proc. Natl. Acad. Sci. USA 97 (2000) 7237.

[23] R. Nifosi, A. Ferrari, C. Arcangeli, V. Tozzini, V. Pellegrini, F. Bertram, J. Phys. Chem. B 107 (2003) 1679.
[24] T.M.H. Creemers, A.J. Lock, V. Subramaiam, T.M. Jovin, S. Voelker, Nat. Struct. Biol. 6 (1999) 557.
[25] P. Schwille, S. Kummer, A.A. Heikal, W.E. Moerner, W.W. Webb, Proc. Natl. Acad. Sci. USA 95 (1999) 151.
[26] A. Voityuk, M.E. Michel-Beyerle, N. Rösch, Chem. Phys. 231 (1998) 13.
[27] A. Voityuk, M. Michel-Beyerle, N. Rösch, Chem. Phys. Lett. 296 (1998) 269.
[28] W. Weber, V. Helms, J. McCammon, P. Langhoff, Proc. Natl. Acad. Sci. USA 96 (1999) 6177.
[29] O. Vendrell, R. Gelabert, M. Moreno, J.M. Lluch, Chem. Phys. Lett. 396 (2004) 202.
[30] M. Martin, F. Negri, M. Olivucci, J. Am. Chem. Soc. 126 (2004) 5452.
[31] R. Zhang, M. Nguyen, A. Ceulemans, Chem. Phys. Lett. 404 (2005) 250.
[32] W. Domcke, in: W. Domcke, D.R. Yarkony, H. Köppel (Eds.), Conical Intersections, Electronic Structure, Dynamics and Spectroscopy, Advanced Series Physical Chemistry, vol. 15, World Scientific, 2004, W. Domcke p. 395; G. Stock, p. 739.
[33] K. Lukyanov, A. Fradkov, N. Gurskaya, M. Matz, Y. Labas, A.P. Savitsky, M. Markelov, A. Zaraisky, X. Zhao, Y. Fang, W. Tan, S. Lukyanov, J. Biol. Chem. 275 (2000) 25879.
[34] D. Chudakov, A. Feofanov, N. Mudrik, S. Lukyanov, K. Lukyanov, J. Biol. Chem. 278 (2003) 7215.
[35] D. Chudakov, V. Belousov, A. Zaraisky, V. Novoselpov, D. Staroverov, D. Zorov, S. Lukyanov, K. Lukyanov, Nat. Biotechnol. 21 (2003) 191.
[36] P.G. Wilman, J. Petersen, R.J. Devenish, M. Prescott, J. Rossjohn, J. Biol. Chem. 280 (2005) 2401.
[37] V. Martynov, A.P. Savitsky, N. Martynova, P. Savitsky, K. Lukyanov, S. Lukyanov, J. Biol. Chem. 276 (2001) 21012.
[38] M.L. Quillin, D.M. Anstrom, X.S. Shu, S. O'Leary, K. Kallio, D. Chudakov, S.J. Remington, Biochemistry 44 (2005) 5774.
[39] L.A. Gross, G.S. Baird, R.C. Hoffman, K.K. Baldridge, R.Y. Tsien, Proc. Natl. Acad. Sci. USA 97 (2000) 11990.
[40] I.V. Yampolsky, S.J. Remington, V.I. Martynov, V.K. Potapov, S. Lukyanov, K.A. Lukyanov, Biochemistry 44 (2005) 5788.
[41] M.E. Bulina, D.M. Chudakov, N.N. Mudrik, K.A. Lukyanov, BMC Biochem. 3 (2002) 7.
[42] M.T. Neves-Petersen, Z. Gryczynski, J. Lakowicz, P. Fojan, S. Pedersen, E. Petersen, S.B. Petersen, Protein Sci. 11 (2002) 588.
[43] F. Pöllinger, C. Musewald, H. Heitele, M.E. Michel-Beyerle, C. Anders, M. Futscher, G. Voit, H. Staab, Ber. Bunsen. Phys. Chem. 100 (1996) 2076.
[44] F. Malvezzi-Campeggi, M. Jahnz, K.G. Heinze, P. Dittrich, P. Schwille, Biophys. J. 80 (2001) 1776.
[45] M.J. Frisch, G.W. Trucks, H.B. Schlegel, G.E. Scuseria, M.A. Robb, J.R. Cheeseman, V.G. Zakrzewski, J.A. Montgomery Jr., R.E. Stratmann, J.C. Burant, S. Dapprich, J.M. Millam, A.D. Daniels, K.N. Kudin, M.C. Strain, O. Farkas, J. Tomasi, V. Barone, M. Cossi, R. Cammi, B. Mennucci, C. Pomelli, C. Adamo, S. Clifford, J. Ochterski, G.A. Petersson, P.Y. Ayala, Q. Cui, K. Morokuma, D.K. Malick, A.D. Rabuck, K. Raghavachari, J.B. Foresman, J. Cioslowski, J.V. Ortiz, A.G. Baboul, B.B. Stefanov, G. Liu, A. Liashenko, P. Piskorz, I. Komaromi, R. Gomperts, R.L. Martin, D.J. Fox, T. Keith, M.A. Al-Laham, C.Y. Peng, A. Nanayakkara, C. Gonzalez, M. Challacombe, P.M.W. Gill, B. Johnson, W. Chen, M.W. Wong, J.L. Andres, C. Gonzalez, M. Head-Gordon, E.S. Replogle, J.A. Pople, Gaussian 98 Revision A.7, Gaussian Inc., Pittsburgh, PA, USA, 1998.
[46] T. Laino, R. Nifosi, V. Tozzini, Chem. Phys. 298 (2004) 17.
[47] C. Scharnagl, R.A. Raupp-Kossmann, J. Phys. Chem. B 108 (2004) 477.
[48] X. He, A.F. Bell, T.J. Tonge, FEBS Lett. 549 (2003) 35.
[49] T.A. Schüttrigkeit, Ph.D. Thesis, TU München, 2004.
[50] M. Prescott, M. Ling, T. Beddoe, A. Oakley, S. Dove, O. Hoegh-Guldberg, R. Devenish, J. Rossjohn, Structure 11 (2003) 275.
[51] J. Petersen, P. Wilmann, T. Beddoe, A. Oakley, R. Devenish, M. Prescott, J. Rossjohn, J. Biol. Chem. 278 (2003) 44626.
[52] J. Wiedenmann, A. Schenk, C. Rocker, A. Girot, K. Spindler, G. Nienhaus, Proc. Nat. Acad. Sci. USA 99 (2002) 11646.